



ELSEVIER

Journal of Power Sources 92 (2001) 267–271

JOURNAL OF  
POWER  
SOURCES

www.elsevier.com/locate/jpowersour

# Measurement of the electrochemical oxidation of organic electrolytes used in lithium batteries by microelectrode

Minato Egashira\*, Hideki Takahashi, Shigeto Okada, Jun-ichi Yamaki

*Institute of Advanced Materials Study, Kyushu University, Kasuga, Fukuoka 816-8580, Japan*

Received 14 April 2000; received in revised form 10 July 2000; accepted 31 July 2000

## Abstract

The electrochemical oxidation of organic electrolytes was investigated using microelectrodes. The electrolytes we used were  $\text{LiClO}_4/(\text{EC} + \text{DEC})$  and  $\text{LiPF}_6/(\text{EC} + \text{DEC})$  which are widely employed in lithium ion batteries. We measured the oxidation current by the potential step method (the potential is maintained until the current becomes constant) at potentials ranging from 4.5 to 5.5 V versus  $\text{Li}/\text{Li}^+$ . The current density–potential relationship of the oxidation of 1 M  $\text{LiClO}_4/(\text{EC} + \text{DEC})$  electrolyte on the carbon microelectrode shows good reproducibility and roughly fits exponential lines. We obtained a similar relationship regardless of the material and size of the microelectrodes. Therefore, the electrochemical oxidation of organic electrolytes can be compared using this method. The different oxidation behavior of  $\text{LiPF}_6$  salt and  $\text{LiClO}_4$  salt electrolyte suggests that the salt anions may initiate the electrolyte oxidation. © 2001 Elsevier Science B.V. All rights reserved.

**Keywords:** Lithium battery; Organic electrolyte; Electrochemical oxidation; Microelectrode

## 1. Introduction

Organic electrolytes, which are produced by dissolving a salt in non-aqueous solvent, have become increasingly important for use in high power density devices, such as lithium batteries.  $\text{LiPF}_6$  is often used as the salt and a mixture of cyclic and linear carbonates (e.g. ethylene carbonate (EC) and dimethyl carbonate (DMC)) is used as the solvent because of their advantages in terms of ionic conductivity and electrochemical stability, especially as regards electrochemical oxidation. When a higher voltage cathode such as  $\text{LiNiVO}_4$  [1] or  $\text{Li}_2\text{CoMn}_3\text{O}_8$  [2] is selected, the stability of the organic electrolyte against oxidation determines the voltage limit of the whole system. Therefore, it is very important to study the oxidation behavior of such organic electrolytes.

The oxidation behavior of various organic electrolytes has been investigated using both spectroscopic [3–5] and electrochemical [6–10] methods. Kanamura et al., confirmed the anodic oxidation of propylene carbonate(PC)-based electrolytes by means of in situ Fourier transform infrared spectroscopy (FT-IR) and X-ray photoelectron spectroscopy (XPS)

[3]. Eggert et al. succeeded in separating the oxidation current of 1 M  $\text{LiClO}_4/\text{PC}$  into solvent and salt contributions using on line mass spectroscopy [4]. However, the ease of electrochemical measurement makes it preferable to these spectroscopic techniques. The oxidation potential can be determined electrochemically in two ways. In one approach, the oxidation potential of a given electrolyte is determined as that at which an applied current density reaches a given threshold value [6,7]. In the other approach, an extrapolated line is drawn along the potential sweep wave (as shown in Fig. 1), and the intersection of this line and the  $i = 0$  line is regarded as the oxidation potential [8–11]. Although the threshold current is different in each report, the former method appears to be better than the latter for the following reason. When the charge-transfer process dominates the whole Faradaic current, the current density–potential relationship of the irreversible oxidation processes of electrolytes must be described by the following Butler–Volmer type equation [12],

$$i = nFC_s k^0 \exp\left[\frac{(1-\alpha)nFE}{RT}\right] \quad (1)$$

where  $i$  is the flowing current density (positive on oxidation),  $n$  the number of electrons associated with the reaction,  $F$  the Faraday constant,  $k^0$  the rate constant of the reaction,  $C_s$  the surface concentration of the reactant,  $\alpha$  the transfer

\* Corresponding author. Tel.: +81-92-583-7790.  
E-mail address: minat206@cm.kyushu-u.ac.jp (M. Egashira).

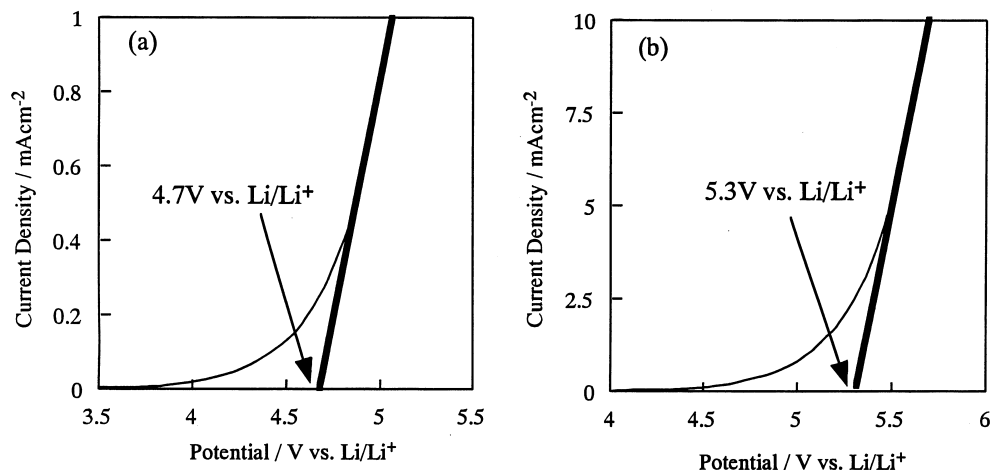


Fig. 1.  $i$ - $E$  curves of the oxidation of the same organic electrolyte with different  $i$  scales, if Eq. (1) can be applied to the oxidation of these electrolytes.

coefficient,  $R$  the gas constant,  $T$  the temperature, and  $E$  is the potential. If the obtained current density is very small compared with the limiting current density,  $C_s$  can be assumed to be the bulk concentration of the reactant. Thus, the Tafel plot ( $\log i$ - $E$  relationship) of this measurement is a straight line. In this  $i$ - $E$  relationship, the intersection moves following the change in the  $i$  range. For instance, while both Fig. 1(a) and (b) show  $i$ - $E$  curves for the same equation, the  $E$  value of the intersection is quite different. Thus, the oxidation potentials obtained by these methods may vary with the experimental apparatus and conditions, and cannot be compared with each other.

In this study, we measure the current density flowing at microelectrodes in organic electrolytes used for commercially available lithium ion batteries toward a given potential, in order to confirm the relationship between current density and potential during the electrochemical oxidation of these electrolytes without the influence of double layer capacitance. A microelectrode has several advantages [13]. These include: (a) it being difficult to reach the diffusion-limited step because of the fast motion of the reactant and product at the electrode surface due to spherical diffusion, (b) the smaller change in the electrolyte composition because the total decomposition is smaller, and (c) the fact that only a small sample is required.

## 2. Experimental

The microelectrode we used in this study (NTT Advanced Technology Corp.) was prepared by using a sputtering method and a mask in a way similar to LSI preparation. As shown in Fig. 2, a carbon or platinum pattern was formed on a glass plate and then a silicon nitride insulation film with a small hole in it (5 and 10  $\mu\text{m}$  in diameter in this study) was sputtered onto it. Lithium foil (Honjo Metal) was cut into squares of about 5 mm  $\times$  5 mm and used as a counter

electrode. We did not use a reference electrode because the size of the microelectrode meant that the applied current was small enough for us to ignore the  $iR$  loss [13]. We confirmed that the overpotential contribution was negligible by comparing our data with 2- and 3-electrode system data. The organic electrolytes we used here were 1 M  $\text{LiClO}_4/(\text{EC} + \text{DEC})(1:1)$  and 1 M  $\text{LiPF}_6/(\text{EC} + \text{DEC})(1:1)$  (Mitsubishi Chemical Corp.). The water content of these electrolytes was kept below 50 ppm, and this was confirmed by measurements obtained with a Karl-Fischer aquacounter (Hiranuma, AQ-7). The potential of the working electrode was raised stepwise from 4 V to about 5.6 V (in 1 M  $\text{LiClO}_4/(\text{EC} + \text{DEC})$ ) or 6.2 V (in 1 M  $\text{LiPF}_6/(\text{EC} + \text{DEC})$ ) by using a highly sensitive potentiostat (Fuso Electric, SECS-318C) connected to a function generator (Hokuto Denko, HB-104). When the potential was set at a certain value (e.g. 5.6 or 6.2 V), a large current (above 10  $\text{mA cm}^{-2}$  at current density) flowed after a few minutes, then the current increased with time at a certain potential and steady-state current did not appear probably due to the decomposition of the silicon nitride layer. Therefore, we did not measure above that potential. The potential was maintained until the applied

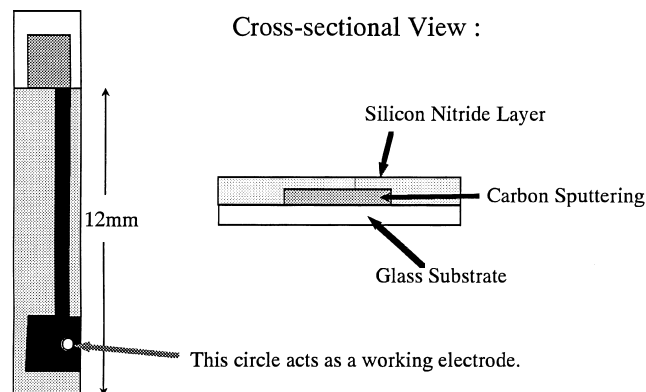


Fig. 2. Microelectrode used in the present study.

current reached a steady state to remove the double-layer capacitance contribution. All the measurements were undertaken in an Ar filled glove box where the atmospheric water content was kept below 1 ppm.

### 3. Results and Discussion

Fig. 3 shows the relationship between the potential and the anodic current density flowing at the carbon microelectrode (5 mm in diameter) in 1 M LiClO<sub>4</sub>/(EC + DEC) solution on a log scale. The potential was stepped anodic to 5.5 V versus Li/Li<sup>+</sup> and then cathodic. Fig. 3 shows the relationship for two cycles. After the first anodic step, all the plots appear to lie roughly on the same straight line although there are small plateaus at 4.8 V. The origin of the deviation observed in the 4–4.5 V region in the first anodic step may be the decomposition of impurities. The reaction that these currents represent seems to be governed by the charge transfer control in this potential range and the electrode surface may not suffer the irreversible degradation. When the potential was raised above 5.5 V versus Li/Li<sup>+</sup> stepwise, the applied current increased with time and no reversibility was observed in the cathodic step. The silicon nitride film may be broken at this potential.

Fig. 4 shows the relationship between potential and oxidation current density on a log scale of a 1 M LiClO<sub>4</sub>/(EC + DEC) solution. We used carbon microelectrodes 5 (a) and 10 mm (b) in diameter and a platinum electrode 10 mm in diameter (c) as working electrodes. When the electrode material was replaced with platinum, the order of the oxidation current densities was similar to that when using carbon electrodes. The log *i*–*E* relationships also seem to lie roughly along a similar straight line regardless of the size and material of the microelectrode.

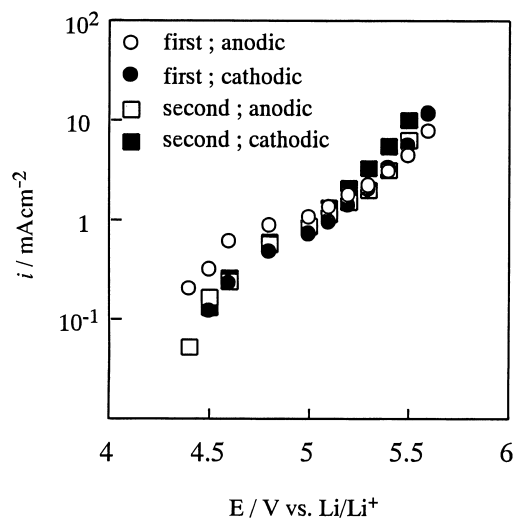


Fig. 3. *i*–*E* relationship of the anodic oxidation of 1 M LiClO<sub>4</sub>/(EC + DEC) electrolyte in two cycles. Microelectrode: carbon, 5 μm in diameter.

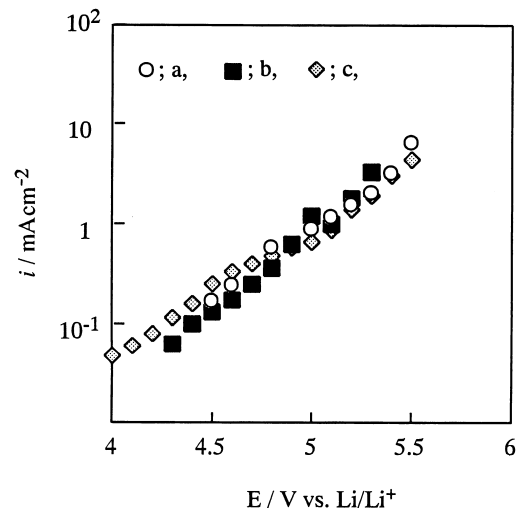


Fig. 4. *i*–*E* relationship of the anodic oxidation of 1 M LiClO<sub>4</sub>/EC+DEC electrolyte. Microelectrode: (a) carbon, 5 mm; (b) carbon, 10 μm; (c) platinum, 10 μm in diameter.

Fig. 5 shows the log *i*–*E* relationships of the oxidation of 1 M LiPF<sub>6</sub>/(EC + DEC) together with that of 1 M LiClO<sub>4</sub>/(EC + DEC) for comparison. With 1 M LiPF<sub>6</sub>/(EC + DEC) electrolyte, the log *i* also has an almost linear relationship with *E*. Ue et al. [7] reported that an electrolyte containing LiPF<sub>6</sub> has a higher oxidation potential than one containing LiClO<sub>4</sub>. The result shown in Fig. 4 seems to contradict that claim at potentials below 5.2 V. These differences may lead to differences in the current density and surface area of working electrodes, or difference in the impurities in the electrolytes.

Fig. 6 shows the log *i*–*E* relationships of the oxidation of 1 M LiClO<sub>4</sub>/(EC + DEC) when *i* was measured with a potential step (a) and potential sweep at a sweep rate of

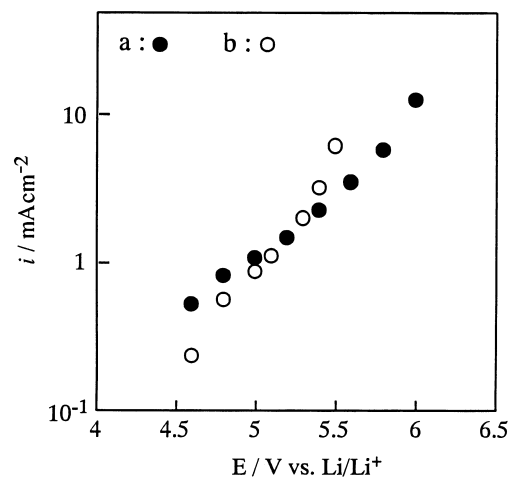


Fig. 5. *i*–*E* relationship of the anodic oxidation of various organic electrolytes. Electrolyte: (a) 1 M LiPF<sub>6</sub>/(EC + DEC)(1:1); (b) 1 M LiClO<sub>4</sub>/(EC + DEC)(1:1). Microelectrode: carbon, 10 μm in diameter.

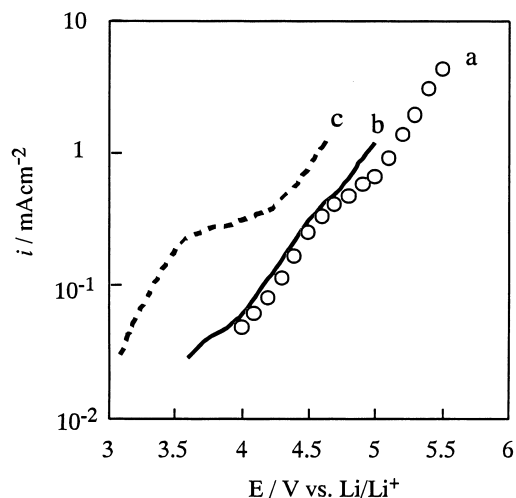


Fig. 6.  $i$ - $E$  relationship of the anodic oxidation of 1 M  $\text{LiClO}_4/\text{EC} + \text{DEC}$  electrolyte. Method: (a) potential step; (b) potential scan rate,  $0.2 \text{ mV s}^{-1}$ ; (c) potential scan rate,  $2 \text{ mV s}^{-1}$ . Microelectrode: platinum,  $10 \mu\text{m}$  in diameter.

$0.2 \text{ mV s}^{-1}$  (b) and  $2 \text{ mV s}^{-1}$  (c). With the slow scan rate, the resulting line provides a good fit with the resulting line of the potential step. The log  $i$ - $E$  line is at a higher position at a faster potential scan because of non-Faradaic currents such as the larger charging currents of the double-layer, and the decomposition of impurities.

The charge transfer processes of electrolyte oxidation seem to limit the whole reaction rate over wide potential ranges such as 4.5–5.5 V versus  $\text{Li/Li}^+$  because the current densities changed roughly exponentially in relation to the potentials. These results indicate that the electrolyte oxidation processes are apparently irreversible making it difficult to determine the equilibrium oxidation potentials of organic electrolytes. In addition, by employing a widely used extrapolation method from a region where a large current flows to the zero current point, we obtained a different oxidation potential for the same electrolyte if the current ranges were different, as mentioned in our Introduction. Therefore, we propose that the oxidation behavior of organic electrolytes should be discussed in terms of all the features of the log  $i$ - $E$  relationship, as shown in Fig. 5, rather than ‘oxidation potential’. If a certain value is required for practical purposes, it is preferable to define the oxidation potential of an electrolyte at a certain threshold current density. The value of the threshold current density should be determined on the basis of a practical case. One example might be where a certain ratio of electrolyte is expected to decompose in a certain time in a commercial AA-type cell. If the size of the electrodes and the amount of electrolyte are estimated to be 240 and  $2 \text{ cm}^2$ , and the expected decomposition rate is  $50 \text{ wt.}\% \text{ h}^{-1}$ , the calculated current density would be  $0.11 \text{ mA cm}^{-2}$ . When this threshold value is applied, the oxidation potentials of 1 M  $\text{LiClO}_4/(\text{EC} + \text{DEC})$  and 1 M  $\text{LiPF}_6/(\text{EC} + \text{DEC})$  are about 4.4 V versus  $\text{Li/Li}^+$  and 3.9 V versus  $\text{Li/Li}^+$ , respectively.

The reaction pathway of the electrochemical oxidation of organic electrolytes has been proposed from several experimental aspects. For example, Arakawa et al. [14] analyzed the oxidation product of 1 M  $\text{LiClO}_4/\text{PC}$  by GC-MS and proposed a two step reaction; first the anion is oxidized electrochemically into a radical species, which then attacks the solvent molecules and converts it into decomposition products, such as propanal. We have not established an experimental basis for understanding the reaction pathway. The small slope of the low  $i$ - $E$  relationship in Figs. 3–5 indicates a small transfer coefficient value (below 0.1) if the whole reaction occurs during one electrochemical process. The low slope may indicate that the oxidation of electrolyte occurs by two step and we have observed the current containing the contribution of a certain mass transfer step. The plateau observed around 4.5 V in Fig. 3 can be interpreted to a multi-step reaction pathway, such as solute decomposition step and solvent decomposition step. Another possibility is the passivation of electrode surface. Aurbach et al. proposed that a surface layer was also generated onto the surface of  $\text{LiNiO}_2$  positive electrode during charge-discharge cycling similar to the passivation layer of negative electrodes, namely SEI [15]. Such layer may form gradually on the microelectrode surface, which prevent the electron transfer by electrolyte decomposition and lower the decomposition current. However, we have no further data to confirm the formation of passivation layer onto the Pt microelectrode used in this study. Further studies that confirm the influences of solute species, temperature and concentration are expected to provide suggestions as to the precise mechanism of the electrochemical oxidation of organic electrolytes.

#### 4. Conclusion

Potential step measurements using microelectrodes show that the current density-potential relationships of the electrochemical oxidation of 1 M  $\text{LiClO}_4/(\text{EC} + \text{DEC})$  and 1 M  $\text{LiPF}_6/(\text{EC} + \text{DEC})$  organic electrolytes provide a rough fit with the exponential curve regardless of the size and material of electrode. These results reveal that the electrochemical oxidation process of an organic electrolyte may be totally irreversible. Therefore, all the features of current density-potential relationship are required when the oxidation behavior of organic electrolytes is compared.

#### Acknowledgements

This work is supported by NTT Telecommunications Energy Laboratories (Nippon Telegraph and Telephone Corporation), Mitsubishi Chemical Corporation, and Industrial Science Research Promotion Foundation. The authors thank Mitsubishi Chemical Corporation for providing the electrolytes used in this work.

**References**

- [1] G.T.-K. Fey, W. Li, J.R. Dahn, J. Electrochem. Soc. 141 (1994) 2279.
- [2] H. Kawai, M. Nagata, H. Tsukamoto, A.R. West, J. Mater. Chem. 8 (1998) 837.
- [3] K. Kanamura, S. Toriyama, S. Shiraiishi, Z. Takehara, J. Electrochem. Soc. 142 (1995) 1383.
- [4] G. Eggert, J. Heitbaum, Electrochim. Acta 31 (1986) 1443.
- [5] B. Rasch, E. Cattaneo, P. Novák, W. Vielstich, Electrochim. Acta 36 (1991) 1397.
- [6] H.H. Horowitz, J.I. Habermann, L.P. Klemann, G.H. Newman, E.L. Strogryn, T.A. Whitney, in: H.V. Venkatesetty (Ed.), Lithium Batteries, The Electrochemical Society Proceedings Series, Pennington, NJ, 1981, p. 131.
- [7] M. Ue, M. Takeda, M. Takehara, S. Mori, J. Electrochem. Soc. 144 (1997) 2685.
- [8] K. Hayashi, S. Tobishima, H. Arai, J. Yamaki, in: Proceedings of the 35th Battery Symposium in Japan, Nagoya, Japan, 1994, p. 151.
- [9] C.W. Walker Jr., J.D. Cox, M. Salomon, J. Electrochem. Soc. 143 (1996) L80.
- [10] J. Barthel, R. Buestrich, E. Carl, H.J. Gores, J. Electrochem. Soc. 143 (1996) 3572.
- [11] S.S. Zhang, C.A. Angell, J. Electrochem. Soc. 143 (1996) 4047.
- [12] A.J. Bard, L.R. Faulkner, Electrochemical Methods, Wiley, New York, 1980, p. 257.
- [13] K. Aoki, Electroanalysis 5 (1993) 627.
- [14] M. Arakawa, J. Yamaki, J. Power Sources 54 (1995) 250.
- [15] D. Aurbach, K. Gamolsky, B. Markovsky, G. Salitra, Y. Gofer, U. Heider, R. Oesten, M. Schmidt, J. Electrochem. Soc. 147 (2000) 1322.